EUROPEAN ORGANIZATION FOR NUCLEAR RESEARCH
European Laboratory for Particle Physics

Large Hadron Collider Project

LHC Project Report 139

Supporting System for the LHC Cold Mass

M. Mathieu, T. Renaglia, C. Disdier*

Abstract

This note summarises the development work carried out on the supporting system for the LHC magnets since 1992. Various technical systems were assessed with variations in the materials, manufacturing methods and dimensions. The assessment concerned both the mechanical and thermal performance. Finally, a recommendation is made for the mass-produced LHC components.

EST
* Doctorate student at the ESIGEC (University of Savoy)

Administrative Secretariat
LHC Division
CERN
CH - 1211 Geneva 23
Switzerland

Geneva, 1 October 1997

CONTENTS

1. INTRODUCTION

CERN is preparing to build a new particle accelerator, the LHC, scheduled for commissioning in 2005. About 2,000 superconducting magnets, which are essential components of this accelerator, will operate with their cold mass at a temperature of 1.8 K. The LHC is described in a report written at the end of 1995 under the title "The Large Hadron Collider Conceptual Design" [1].

The magnet cold mass is to be supported by composite material components called **"cold feet"** providing the transition between the temperature of 1.8 K and ambient temperature.

This note gives an account of the development work made on these components over the past 4 years, terminating in a recommendation for the manufacture of the supports to be fitted in the accelerator.

2. INITIAL SPECIFICATION

2.1 General

The supporting system must ensure the positional stability of the LHC magnets in their cryostats.

There are two types of magnets to be considered : dipoles 15 metres long with a mass of 27,000 kg or quadrupoles 3 metres long with a mass of 6,000 kg.

In addition, the feet must minimise heat transfers from the hot to the cold regions to prevent excessive helium consumption (see section in Appendix 1).

Only one foot of each component is fixed, while the others can slide (or move) to allow for the movement caused by the contraction of the magnets during cooling.

2.2 Mechanical characteristics

The mechanical characteristics are set out in the table in Appendix 2 and the sketch in Appendix 3 relates to the values specified at the start of the project.

They have changed since 1991 [2], since, at the start of the project, 2 feet supported a magnet 10 m long with a mass of 20,000 kg, whereas now 3 feet support a magnet 15 m long with a mass of 27,000 kg.

The lateral force of 50 kilonewtons on the fixed foot of the quadrupole acts only during assembly when warm : in certain configurations there is a vacuum in one region and atmospheric pressure in the neighbouring one, giving rise to a force caused by the pressure difference of 1 bar on either side. The component separating the two regions is called the **"vacuum barrier"**.

The lateral force on the movable foot of the dipole depends on the coefficient of friction between the bottom of the foot and its seat on the vacuum chamber. The figures specified at the end of 1996 will be found in Appendix 4.

2.3 Thermal characteristics

The heat transfer between the surroundings at 300 K and the cold mass at 1.8 K must be minimal.

The values at the various temperature levels are given in Appendix 2. The requirements increased substantially between 1992 [3] and 1996 in line with the technical progress made. The latest are given in Appendix 4.

3. REVIEW OF THE COMPONENTS TESTED AT CERN

3.1 Filament winding (Appendix 5)

20 prototypes based on a filament winding technique were built.

The structural part of the foot is a cylinder with an 8-layer filament winding wound on a tube.

The fibre is conventional glass fibre and the matrix is an epoxy resin. The equivalent thickness of the cylinder is 6 mm. The glass fibre filling rate is excellent and can be as high as 77% by mass. The two intermediate flanges (4.5 K and 77 K levels) supporting the heat screen and the super-insulation are aluminium as here good heat conductivity is required.

All the flanges are adhesively secured to the wound cylinder. These first-generation prototypes were fitted in the test cell SM18 (String 1) and have been operating for nearly two years.

The mechanical characteristics of the wound cylinder as given by the manufacturer are high (E = 32 GPa, UTS about 400 MPa).

3.2 Glass drape (Appendix 6)

After fitting the above feet to the various prototype magnets, we ordered various components from industry using several different technologies within the composite material field.

The drape technology (common in the aeronautical industry) consists in taking glass cloth pre-impregnated with epoxy resin, shaping it on a mould which may itself be made of composite material and putting it into an autoclave at about 120°C to polymerise it. The glass fibre filling rate is about 65% by mass.

The component may be fairly complex in shape as draping is done by hand. The mould is not very expensive as it is not subjected to high pressures; labour costs, however, are fairly high.

The lower and upper flanges are also made of glass composite integrated into the moulded component. Threaded metal inserts for securing purposes are embedded in the flanges before entry into the autoclave. The aluminium screen support flanges are adhesively secured to the cylinder.

A foot of this type has been bought and tested at CERN.

The mechanical characteristics are slightly below those of the filament winding owing to the lower fibre filling rate (E = 24 GPa, UTS about 300 MPa).

3.4 Glass/carbon drape (Appendix 7)

The manufacturing process is the same as for the previous foot. However, the material is glass fibre for the bottom of the foot (77 K level) and carbon fibre for the top (1.8 and 4.5 K level).

Carbon fibre is used on account of its very low heat conductivity in the 2 to 40 K range.

The delicate feature of this structure is the strength of the adhesive bond between the carbon and glass sections. The difference between the coefficients of heat contraction of the two materials is 1.5 mm/m in the range of 2 to 300 K.

Four feet of this type were made by industry and tested at CERN.

3.4 Resin Transfer Moulding (Appendix 8)

The resin transfer moulding manufacturing process, commonly called RTM, differs from the one above as it uses dry glass cloth.

The dry cloth is inserted into a metal mould capable of withstanding considerable forces.

Epoxy resin is then injected under pressure through an aperture to fill all the spaces. The whole is then polymerised at 140°C, after which the mould is dismantled to extract the component.

Here, too, the upper and lower flanges are made of glass composite integrated into the moulding. Metal inserts are fitted in the flanges at the time of moulding. The copper screen-support flanges are adhesively secured to the cylinder.

Three identical RTM components were made by the Spanish aeronautical industry under a co-operation contract with CERN [4].

3.5 Filled thermoplastics

3.5.1 General

The previous components are all made from a heat-curing resin (an irreversible process) reinforced by glass or carbon fibre.

In order to test a radically different technology, we ordered glass-fibre reinforced thermoplastic resin (a reversible process) cold feet from industry. A great deal of progress has, in fact, been made in the field of thermoplastics over the past six years and even the resins alone have good mechanical properties.

Here, the basic product takes the form of solid granulates which are injected at a pressure which may be as high as between 1200 and 1800 bars and heated to a high temperature (400°C) during the process.

The component solidifies very quickly on contact with the mould, which is then opened to recover the component.

The mould is very expensive, for it must be made to a high degree of mechanical precision (finished moulding) and must be very strong owing to the high pressures involved.

The glass fibres are very short and are randomly oriented in the finished product. We tested various thermoplastics, all reinforced with glass fibres.

3.5.2 ULTEM® 2300[*] (Appendix 9)

This product is a glass-fibre-reinforced polyether imide with good mechanical properties (E = 9 GPa, UTS = 160 MPa).

It has been used in the United States for supports for the prototype quadrupole magnets of the SSC (3 feet per 5-tonne magnet) [5] [6].

To minimise the cost of the mould we designed a simple shape and 6 feet were made by a Dutch firm at the beginning of 1995.

3.5.3 ISARYL® 15

ISARYL® 15 is a polyarylate with good mechanical properties as the resin alone has E = 2.5 GPa, UTS = 90 MPa at ambient temperature [7] [8].

The resin is reinforced with glass fibre (40% of the total mass) to make the cold foot.

The ultimate tensile stress at ambient temperature was found to be 130 MPa in the measurements made at CERN. The figure is 280 MPa at liquid nitrogen temperature.

---

[*] Registered trade mark of General Electric Plastics

An order for six components was placed at the end of 1994 with an Austrian firm, but manufacture of the product was forbidden in Austria at the beginning of 1995 for environmental protection reasons.

Fortunately, the Dutch firm which had made the six ULTEM® components was also able to make us six of ISARYL® using the same mould in June 1995.

3.5.4 ULTRAPEK®[**]

ULTRAPEK® is a polyaryl ether ketone also known as PEEK (E = 12 GPa, UTS = 185 MPa) [9].

It is used in the aeronautical industry and may be used as a replacement for aluminium in certain components.

It has very good mechanical properties which are retained at high temperatures (over 200°C).

The same Dutch firm made us six ULTRAPEK components in June 1995.

4. MECHANICAL STRENGTH CALCULATIONS ON FINISHED PARTS

4.1 Introduction

Alongside the experimental examination of the mechanical behaviour of the prototype supports, we made a few simulations on several types of cold feet in relation to various changes in the cryostat dimensions. The purpose of this analysis was, of course, to quantify the mechanical strength of the prototype before possibly having it manufactured and hence make development more flexible. This parametric study of the problem was made with the MOSAIC computer code (product of FRAMASOFT - FRANCE) in collaboration with the Composite Materials Laboratory of the University of Savoy.

[**] Registered trade mark of BASF

4.2 Prototype examination - Description

In all the mechanical strength calculations quoted here after, the reference used for the various models was prototype C01 (made by COURTAULDS AEROSPACE)[***]. Before going further, we must set out the main features of this prototype (Appendix 5).

- Stainless steel lower and upper flanges.
- Filament-wound tube.
- Tube thickness: e = 6 mm.
- Stacking sequence of the composite material of the tube: (±88°, ±15°).

We used the following simplifying assumption for the calculations : the eight-layer composite material was replaced by a single-layer 6 mm thick, the mechanical characteristics of which are equivalent to those of the composite material. It is then possible, by simply parametrising the tube thickness, to obtain the range of stress inside the cold foot when the tube thickness is reduced from 6 to 4 mm.

4.3 Prototype examination - Results

Owing to the successive modifications in the design of the cryostat, we made models of several different prototypes. The last ones take account of the reduction in the cryostat diameter as a result of the separate cryostat line decision.

The results obtained for these various feet are set out in a table in which the stresses are expressed in MPa (Appendix 10).

These results show that, through this initial approach, the calculated maximum stress levels are clearly lower than the typical ultimate tensile stresses of the composite material. A glass composite made according to normal trade practice has a UTS of 250 to 400 MPa depending on the fibre orientation, the filling ratio, etc. These results are confirmed by a "composite" of foot C01 (considering an eight-layer composite). Appendix 10 gives the conventional values of the strength of the materials obtained for four different types of foot. Appendices 11 and 12 give examples of graphic output for feet 250 mm high, and respectively 6 and 4 mm in thickness.

[***] By the process described in 3.1

The detailed calculations will be published on the occasion of the defence of a thesis at the University of Chambéry by C. Disdier.
Work meanwhile has been the subject of various successive reports referred to at the end of this note [10] [11].

5. THERMAL CALCULATIONS

5.1 General

Account was primarily taken in the thermal calculations of the conduction in the column of insulating material. Thermal radiation is relatively insignificant in the 77 to 2 K range, and the losses recorded are negligible by comparison with losses by conduction.
The energy emitted by radiation from a surface A is given by the Stefan-Boltzmann equation:

$$W_r = \sigma\, e\, A\, T^4,$$

where

W_r = radiated energy in Watts

σ = the Stefan-Boltzmann constant = 5.67×10^{-12} W x cm^{-2} x K^{-4}

e = the emission capacity of the surface A

A = the area of the surface expressed in cm^2

T = the temperature in K.

By way of example, a polished and degreased stainless steel surface (emissivity of 0.06) of 100 cm^2 radiates 1.3 mW at 77 K, which makes it possible to ignore this effect in a first approximation in the 1.8 to 77 K range. For comparison, the same surface at 300 K (emissivity of 0.15) would radiate 700 mW.

5.2 Conduction calculations

The thermal flux in W between two points on a body at temperatures of T_1 and T_2 respectively, is expressed by :

$$P = {}_{T1}\int^{T2} S/L\, \lambda\, (T)\, dT$$

where λ is the heat conductivity of the material and S is the cross-section though which the flux passes over a distance L (with the whole expressed in MKS units) [12].

A calculation made with λ (T) assumed to be equal to the mean between T_1 and T_2 gives :

$$P = S/L\, \lambda_{T1\,T2}\, (T_2 - T_1).$$

We have drawn up a parametrised table making it possible to calculate the losses by heat conductivity with different materials for cylinders of various cross-sections and lengths. The conductivities are taken from the table in Appendix 13 obtained from various cryogenics periodicals [13] [14].

In the calculation table (Appendix 14), the first column of figures is obtained by taking the half-sum of the end figures as a conductivity value and the second column is obtained by integrating the function λ (T), expressed in the form of a 2nd-degree polynomial in T.

The results are fairly close. By way of example, Appendix 14 shows a table with a foot entirely of glass-fibre and in Appendix 15 a table with a foot of carbon fibre in the 1.8 to 4.2 K range and glass-fibre for the higher temperatures.

The figures obtained are compared to the heat loss figures quoted in Appendix 4 of the LHC yellow book [1]. The cold foot's contribution to the losses can thus be assessed.

It is found that the upper carbon part gives very much lower losses than those specified. The glass composite part gives values complying with the specification.

More detailed heat loss calculations including all the components have been made in the Cryogenics group of AT Division [15] and confirm the values given in the attached tables.

6. THE MECHANICAL TESTS

6.1 Tests using the traction machine

6.1.1 Description (drawing in Appendix 16)

This first test on the mechanical strength of the prototype LHC magnet supports makes it possible to study the behaviour of cold feet under axial compression and under flexion.

Here we make use of the traction machine (in bld. 376 - R015) to apply compressive stress to the cold foot. Lateral force is obtained via a device essentially consisting of a rigid column (ref. 1) and a hydraulic ram (ref. 13). The column is inserted inside the foot and firmly secured to the lower flange by the fixing screws provided.

The whole is capped by a cover (ref. 7) secured to the upper flange of the foot through which passes the piston (ref. 7) used to transmit the flexing force.

As the hydraulic ram is rigidly secured to the cover, the piston bears on the central column, assumed to be rigid, to cause the support on test to flex.

Finally, the compressive force is applied by the traction machine's cross-member to the cover (ref. 7). The needle-roller bearing between the cover and the cross-member will then permit the top of the foot to be moved horizontally under the effect of the force transmitted by the hydraulic ram.

Before analysing the results obtained for the various prototypes tested, however, it must be emphasised that this rig does not make it possible to reproduce exactly the conditions of use of the cold foot inside the cryostat.

When the lateral force is applied, in fact, there is nothing to prevent the upper flange of the cold foot from rotating, which would not actually occur owing to the rigidity of the cold mass of the magnet.

By nevertheless allowing this rotation, the component on test will bear more severe stress than when finally fitted in the LHC machine.

Moreover, for the sake of convenience, we conducted this first set of tests only at ambient temperature. It would have been too complicated to equip our traction machine for making mechanical tests at cryogenic temperatures. We therefore elected to make a simplified examination in an initial stage before going on to a full-scale examination of the mechanical behaviour of the cold foot inside the cryostat, which will combine the effects of vacuum, temperature and mechanical stresses.

6.1.2 Results

It was possible to test various prototype feet using this rig. Although this first test is not fully representative of the actual conditions in which the magnet supports will be used, it did, besides the scheduled stress measurements, make it possible to detect any manufacturing or design faults. These include, for instance, an undersize problem in the securing flanges discovered on prototype C21.

The result of this failure was to raise the lower flange between the securing screws under the effect of lateral stress. The measurement of the movement of the top of the foot was therefore incorrect.

This preliminary examination nevertheless allows us to make an initial comparison of the mechanical characteristics of the various prototypes at different loads:

- maximum compressive force Fz = 100 kN, which corresponds to the load to be supported by each foot during normal operation (for a dipole magnet),
- compressive stress Fz = 100 kN combined with a lateral force Fy = 50 kN,
- compressive stress Fz = 26 kN combined with a lateral force Fy = 50 kN (for a quadrupole magnet).

The lateral force, assessed at 50 kN, is caused by the vacuum barrier force when the adjacent cell is gradually evacuated.

The table in Appendix 17 summarises the deflection measurements obtained.

The six strain gauges spaced evenly over the circumference of the bottom of the foot (Appendix 18) make it possible to estimate the maximum stress produced by the flexional force from the results obtained for the pure compression tests.

The result obtained is not strictly accurate because we are unable to obtain the Poisson coefficient by using two gauges at 90°.

To be more precise we could have used a gauge at 45° in addition to the two at 90°, which would have given us access to the Poisson coefficient of the composite material.

The results of the strain measurements are also summarised in the table in Appendix 17, which may be compared to the theoretical values of the UTS of these materials.

Finally, we also made a compression test at 200 kN to ensure that there is a greater safety margin in the strength of the cold feet. None of the feet used broke.

To complete these compression tests, we shall be performing a set of breakage tests in the near future using a press capable of subjecting our components to a maximum force of 300 tonnes.

6.2 Full-scale tests

6.2.1 Description

To supplement the tests made using the traction machine, we then set up a second test rig to approach the actual operating conditions of the superconducting magnet supports more closely.

We deliberately took as a basis the examination of the case of load 3 (compression 26 kN, flexion 50 kN) as corresponding to the most critical stress on the cold foot.

For reasons of cost and convenience, this test rig consists solely of a duralumin girder weighted with lead. It was adopted to avoid the material and labour costs involved in the use of a real magnet at cryogenic temperatures.

Like a magnet, this girder is supported on two feet (Appendix 19), one free to move to allow for the contraction of the girder during cooling and the other fixed, on which the forces simulating the effect of the vacuum barrier are concentrated.

The mass of the magnet is simulated by adding blocks of lead on carriages which can be moved on the beam to concentrate the compressive force on one or other foot, as required.

This thus provides a low-cost test rig faithfully reproducing the mechanical stresses which will be acting on the magnets during the assembly and continuous running of the LHC.

The beam acting as the cold mass of the superconducting magnet is cooled by liquid nitrogen running through a winding pipe fitted to both surfaces of the girder.

Liquid nitrogen is used because the costs involved in the use of superfluid helium as the coolant (pumping system, fitting heavy heat insulation inside the croystat) are not fully justified. The temperature variations in the 1.8 to 77 K range actually change the physical characteristics, at least the coefficients of heat expansion, of the materials used (Appendix 20) only slightly.

6.2.2 *Results*

Over the past two years we have been able to test several prototype LHC superconducting magnet supports representing the various methods of making the composite materials.

All the cold feet listed in the table in Appendix 17 were first subjected to a series of tests using the traction machine (bld. 376-R015).

So far, of all the prototypes tested in our test cell at SM18, only two filled thermoplastic ones have been destroyed by a lateral force of 50 kN, equivalent to the stress imposed by the vacuum barrier.

The first result of this examination is that filled thermoplastic is unsuitable for the LHC dipole magnet supports.

Even though one prototype made of ULTEM[*] (UL2) withstood the tests, the material must be rejected as it is not rigid enough.

Leaving the foot (C01), which is the only prototype with a tube 6 mm thick, out of consideration, the examination of the movement of the tops of the various feet (Appendix 21) confirms that the filament winding system gives a support with the greatest rigidity for equal thickness.

It is also found that the two drape feet (4 mm thick) behave similarly, although the glass cloth is replaced in the upper part of the mixed glass/carbon foot by a carbon fabric with better mechanical properties. The similarity is explained by the fact that this crown is too small to have any real influence on the mechanical behaviour of the foot. This prototype need not therefore be considered, even if the presence of the carbon in the upper part of the foot (2 to 5 K region) substantially improves the foot's thermal properties. Moreover, the cost of a mixed foot is considerably higher than that of one made of a single material.

Finally it is noted that, in the tests performed at cryogenic temperatures, the deflections measured (Appendix 21) at the top of each foot are 10% lower than those recorded during the tests at 300 K. Moreover, the order observed during the tests at ambient temperature remains valid at low temperature.

---

[*] Registered trade mark of General Electric Plastics

7. THERMAL TESTS

7.1 General

The thermal tests were performed in CERN's cryogenics laboratory and are discussed in publications referred to at the end of this note [16], [17], [18]. The cold foot is placed in a cryostat (Appendix 22) making it possible to influence the rated temperature levels at various cooling points. The heat flux from one level to another is measured by means of suitable calorimeters.

This heat flux is compared with a measurement of the quantity of helium evaporated: with the knowledge of the thermal characteristics of the fluid at various temperatures, the quantity of heat dissipated in the helium is obtained.

7.2 Results

The results obtained are shown in the table of Appendix 23. A very good correlation between the calculations and measurements for levels 1.8 to 4.5 K and 4.5 to 77 K will be noted. However, the value measured in the 77 to 293 K range is regularly 1.5 to 2 W above the calculated figure. The difference arises from the heat radiation which was not taken into account in the calculations. Tests have been made to minimise these losses due to radiation by surrounding the base of the foot with aluminised Mylar, resulting in a reduction because of the low emissivity of the material [19].

As will be seen from the table, for the same thickness carbon gives remarkable results (confirming the calculations), and equivalent results for the same thickness are obtained between the various materials (glass composite or glass thermoplastic) for the same temperature levels.

The measurements made in the laboratory confirm the calculations and show that the various technical systems proposed are compatible with the loss levels required in the specification.

By way of a reminder, the final column of the table gives the total heat losses for a dipole cryostat, with an associated separate line, as quoted in the yellow book on the LHC [1].

8. CONCLUSION

With about 30 prototypes using three different technological methods in the field of heat-curing resin composites and 20 prototypes made using three different filled thermoplastic resins, we built and tested a wide sample of components.

The mechanical strength runs in the order below, starting with the maximum: filament winding, cloth drape, Resin Transfer Moulding, filled thermoplastic. The only problem with the filament winding is securing the end flanges, which can be difficult. At the other end, the thermoplastic feet filled with short fibres yielded during the lateral load test.

The heat conductivity tests confirmed the excellent performance of carbon at very low temperatures. However, the glass fibre components give results fully meeting the requirements of the specification. The thermoplastic components, too, display low heat conductivity.

In conclusion, we recommend the use of cold feet for the LHC machine made of composite material using long glass fibres as the reinforcement with a matrix of epoxy resin (method of manufacture: drape or Resin Transfer Moulding), as shown in the drawing of Appendix 24.

9. ACKNOWLEDGMENTS

It has been possible to complete this work owing to the co-operation of many people at CERN essentially on the mechanical side : T. Renaglia for the drawings and C. Disdier, M. Blin and L. Aliu for the tests.

On the thermal side, advice and help with the calculations were provided by P. Lebrun and G. Riddone, while the measurements were made in the cryogenic laboratory of J.M. Rieubland by H. Danielsson, C. Luguet and B. Jenninger.

The prototypes were made by five firms with factories in seven European countries.

LIST OF REFERENCES

[1] The LHC Study Group
The Large Hadron Collider Conceptual Design
CERN/AC/95-05 (LHC) du 20/10/95

[2] M. Mathieu
Specification for the manufacture of composite material support posts for the prototype LHC magnets
DO-11460-LHC, July 1991

[3] Ph. Lebrun
Cahier des charges d'un système de support cryogéniques des aimants LHC dans leurs cryostats
Note AT-CR/PhL du 19/01/90

[4] Contract no F193/MT-LHC - 13/07/92

[5] The qualification and reliability verification of a low cost cryogenic support post for SSC quadrupole magnets.
M. W. Hiller, R.J. Kunz, G. A. Lehmann and M. J. Nilles
Paper IV-2 presented at the Fifth Annual International Industrial Symposium on the Super Collider (IISSC 5)
May 6-8 1993 San Francisco, CA

[6] ULTEM resin Design Guide
General Electric Plastics

[7] High Temperature Polyarylates
Isonova Technische Innovationen GMBH

[8] Tensile, fracture and thermal properties of polyarylates at room and cryogenic temperatures
K. Humer, E.K. Tschegg* and H.W. Weber
Atominstitut der Osterreichischen Universitäten,
A-1020 Vienna, Austria
* Institut für Angewandte und Technische Physik, TU Vienna, A-1040 Vienna, Austria

[9] UltraPek
Hochtemperaturbeständiges Poly(aryletherketon) PAEK
BASF Aktiengesellschaft

[10] Rapport d'activité 1994
C. Disdier / Stagiaire Doctorant de l'Université de Savoie.

[11] Rapport d'activité 1995
C. Disdier / Stagiaire Doctorant de l'Université de Savoie.

[12] Eléments de cryogénie - R.R. Conte - Masson et Cie Editeurs 1970

[13] E.I. Augsburger, W. Dietsche, H. Kinder and J. Becker
Thermal conductivity of several fibres - reinforced composites between 2 K and 300 K
Cryogenics - Nov. 80 , pages 666 à 667

[14] BNL Cryogenics Data Handbook

[15] Contribution to the analysis of the cryogenic thermal budget for the LHC (Large Hadron Collider) project
Germana Riddone - Politecnico di Torino

[16] H. Danielsson, B. Evans
Thermal Evaluation of support post prototypes for the LHC
CERN AT Group Report, 93-02

[17] M. Blin, H. Danielsson, B. Evans and M. Mathieu
Design, Construction and Performance of superconducting magnet support posts for the Large Hadron Collider
Advanced Cryogenics Eng. 39A - 671-678 (1994)

[18] H. Danielsson, Ph. Lebrun and J.M. Rieubland
Precision Heat Inleak Measurements on Cryogenic Components
at 80 K, 4.2 K and 1.8 K
CERN LHC Note 190 - 06/92

[19] Influence of reflecting surfaces on the LHC support posts
B. Jenninger / LHC-ECR / 1996

LHC support post 1997: Appendix list

Appendix 1 : LHC initial cross-section
Appendix 2 : 1992 Technical specification for support post
Appendix 3 : Service loadings conditions
Appendix 4 : 1996 Technical specification for support post
Appendix 5 : Glass Filament winding support post
Appendix 6 : Glass sheet moulded support post
Appendix 7 : Carbon glass sheet moulded support post
Appendix 8 : Resin transfer moulding support post
Appendix 9 : Charged thermoplastic support post
Appendix 10 : Stresses calculations
Appendix 11 : Graphic output thickness 6 mm
Appendix 12 : Graphic output thickness 4 mm
Appendix 13 : Thermal conductivities
Appendix 14 : Thermal losses: Glass fibre post
Appendix 15 : Thermal losses: Carbon/glass fibre post
Appendix 16 : Tension and compression testing machine
Appendix 17 : Stresses and strains : testing machine
Appendix 18 : Strain gauges implementation
Appendix 19 : SM 18 testing machine
Appendix 20 : Thermal contraction of materials
Appendix 21 : Post deflection : SM 18 testing machine
Appendix 22 : Cryostat for thermal tests of posts
Appendix 23 : Thermal measurements overview
Appendix 24 : LHC dipole cross section as in 1996

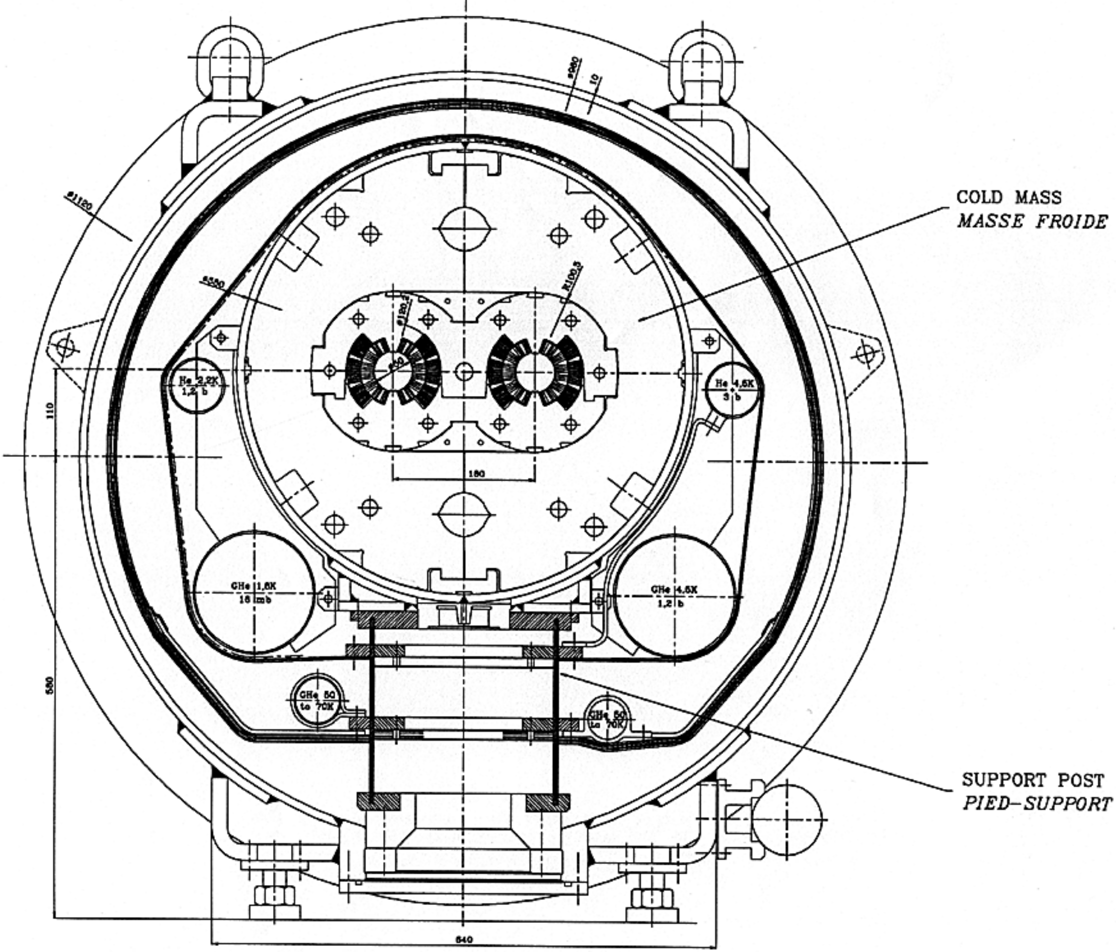

LHC DIPOLE : STANDARD CROSS-SECTION

DIPOLE LHC : COUPE TRANSVERSALE

LHC PROTOTYPE SUPPORT POST

TECHNICAL REQUIREMENTS

MECHANICAL

Loads per post	Dipole	Quadrupole
Axial load (Compressive)	90 kN	26 kN
Maximum Radial load (Lateral)	15 kN	50 kN

MECHANICAL TOLERANCES

Positionning	0.20 mm
Reproducibility	0.05 mm
Angular Upper Plate	0.50 Milliradian

MAXIMUM THERMAL LOSSES

	Watts per post
at 1.8 K	0.1 Watts
at 5 K	1.0 Watts
at 80 K	10.0 Watts

RADIATION LEVEL

	20 years (Grays)
at TOP	1.00E+04 Grays
at BOTTOM	4.00E+02
SPECIFIED	1.00E+06

Appendix 3

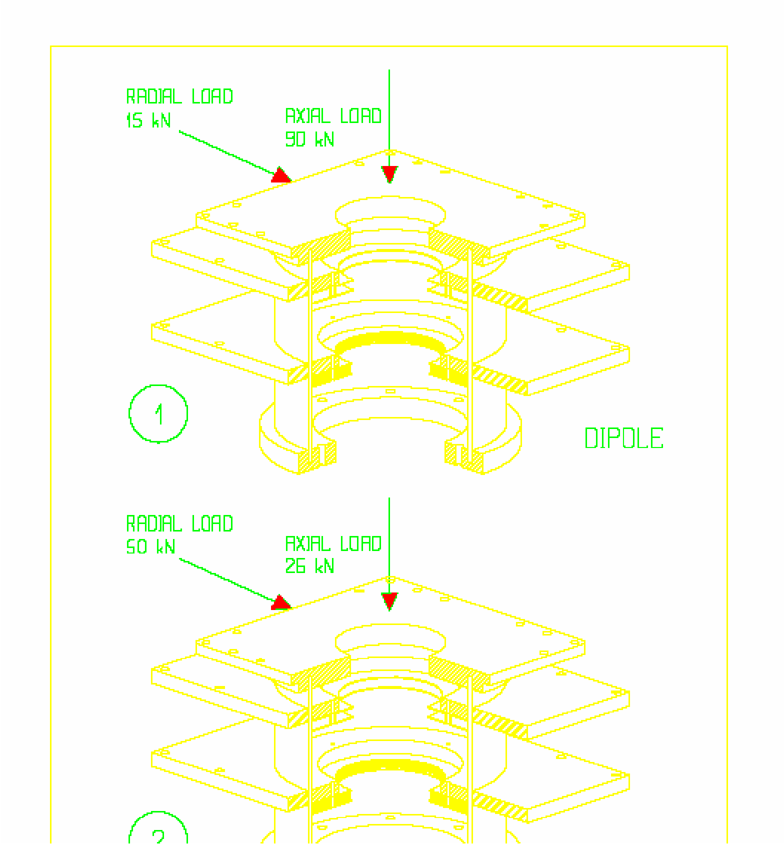
RADIAL LOAD
15 kN
AXIAL LOAD
90 kN
1
DIPOLE
RADIAL LOAD
50 kN
AXIAL LOAD
26 kN
2

LHC PROTOTYPE SUPPORT POST 1996

TECHNICAL REQUIREMENTS

MECHANICAL

Loads per post	Dipole	Quadrupole
Axial load (Compressive)	90 kN	30 kN
Maximum Radial load (Lateral)	36 kN	50 kN

MECHANICAL TOLERANCES

Positionning	0.20 mm
Reproducibility	0.05 mm
Angular Upper Plate	0.50 Milliradian

MAXIMUM THERMAL LOSSES

	Watts per post
at 1.8 K	0.05 Watts
at 5 K	0.50 Watts
at 80 K	5.00 Watts

RADIATION LEVEL

	20 years (Grays)
at TOP	1.00E+04 Grays
at BOTTOM	4.00E+02
SPECIFIED	1.00E+06

Appendix 5

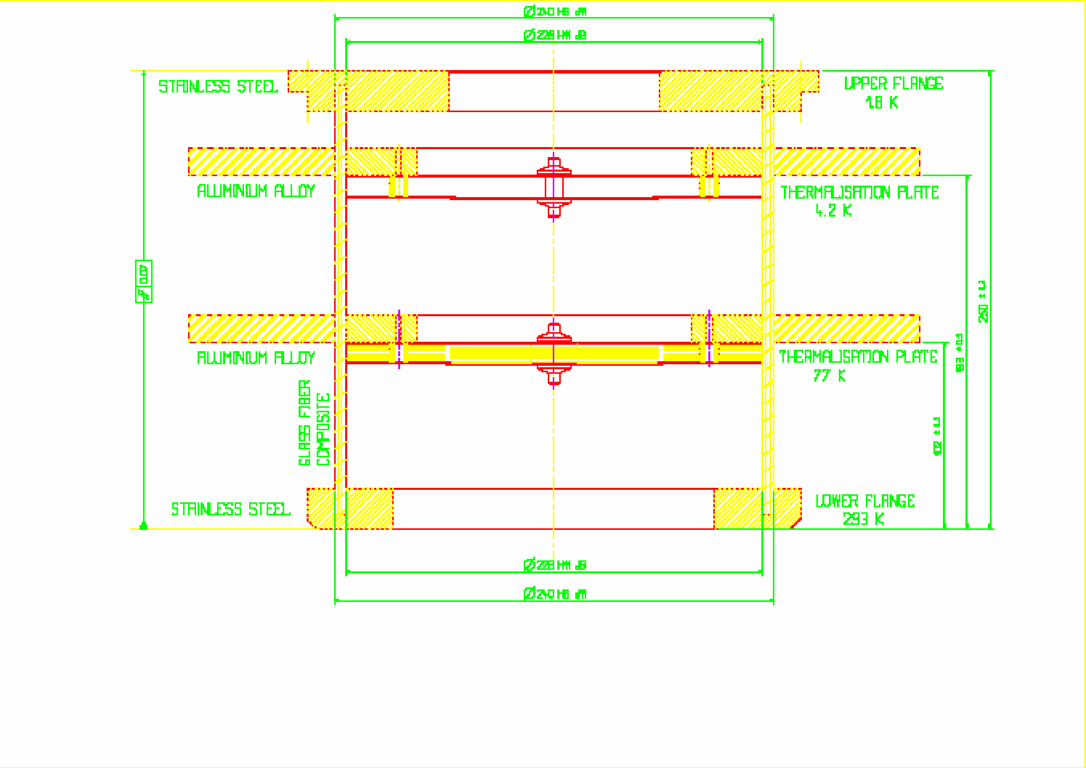
Ø240 H8 d11
Ø228 H11 d8
STAINLESS STEEL
UPPER FLANGE
1.8 K
ALUMINIUM ALLOY
THERMALISATION PLATE
4.2 K
ALUMINIUM ALLOY
THERMALISATION PLATE
77 K
GLASS FIBER
COMPOSITE
STAINLESS STEEL
LOWER FLANGE
293 K
280 ± 0.3
183 ± 0.3
102 ± 0.3
Ø228 H11 d8
Ø240 H8 d11

Appendix 6

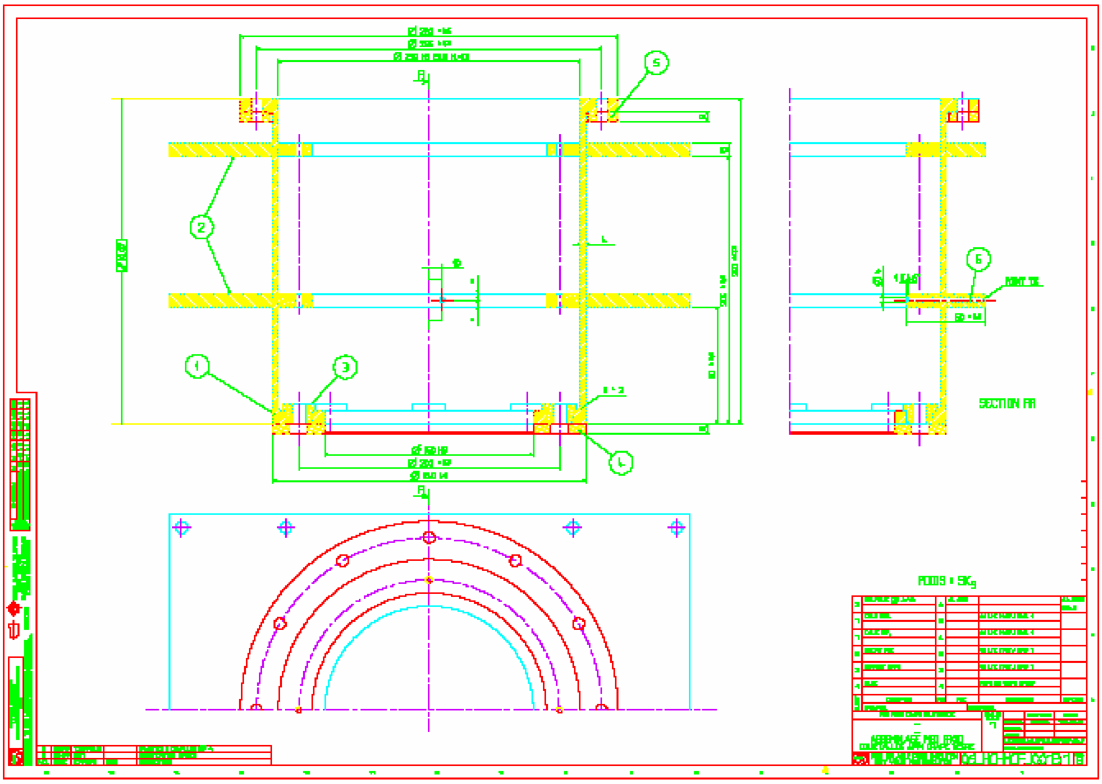

Appendix 7

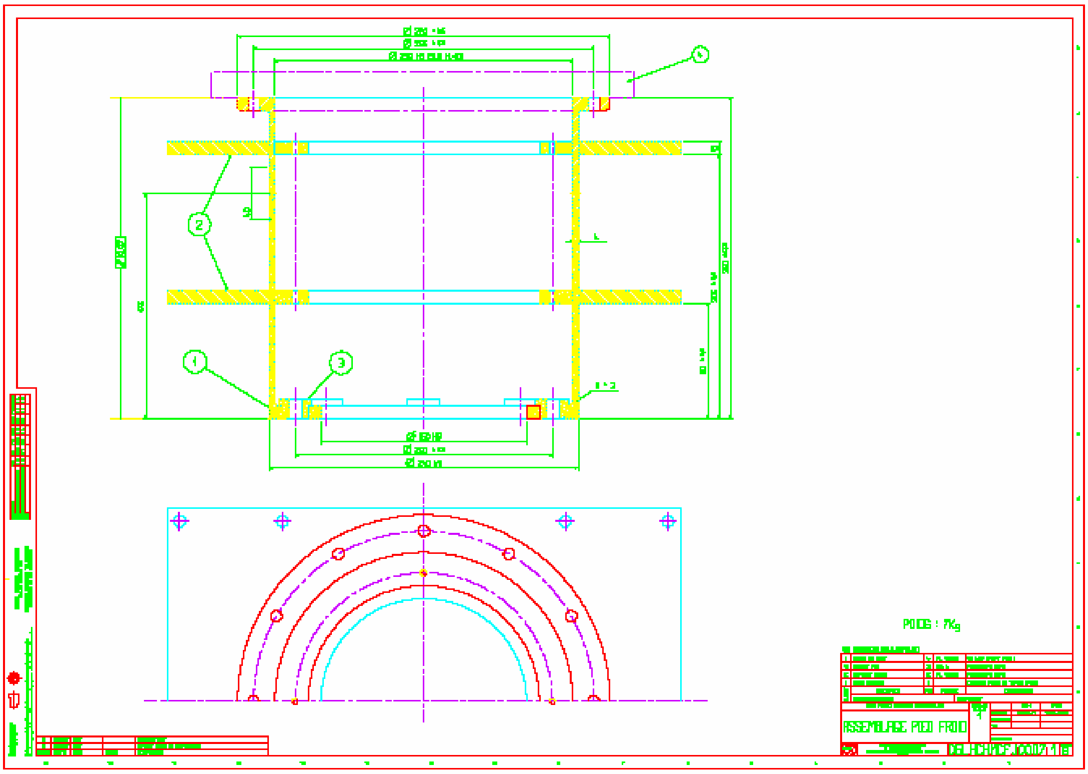

Appendix 8

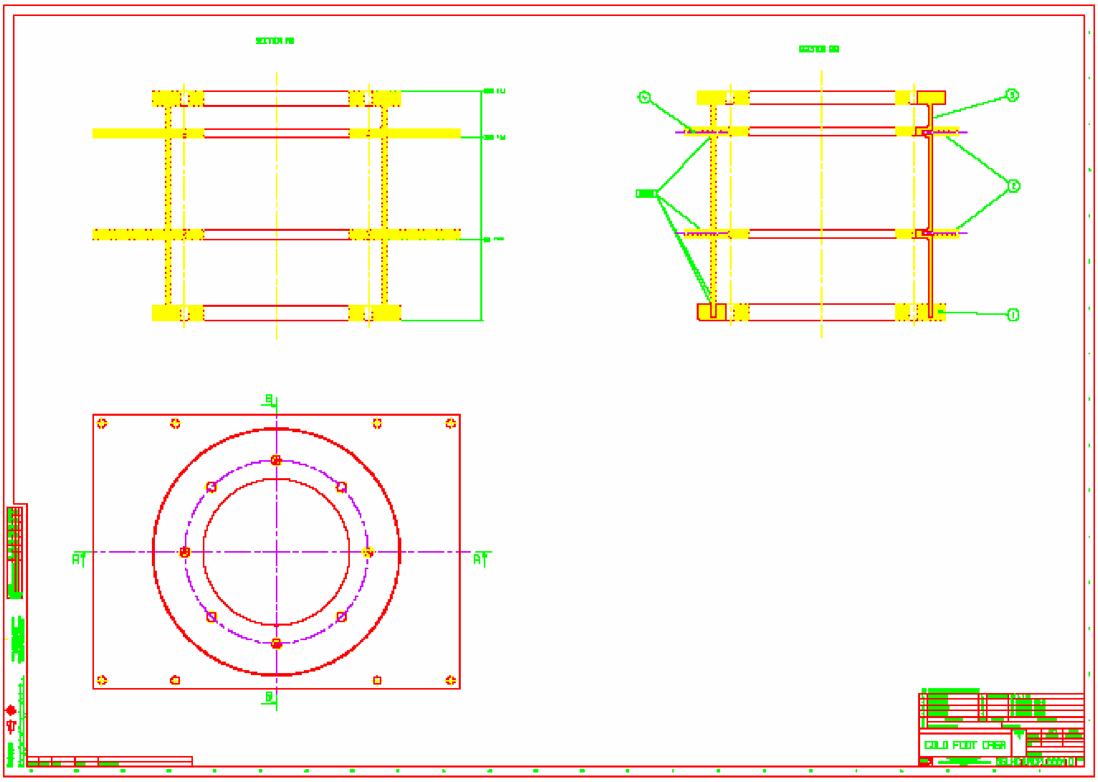

Appendix 9

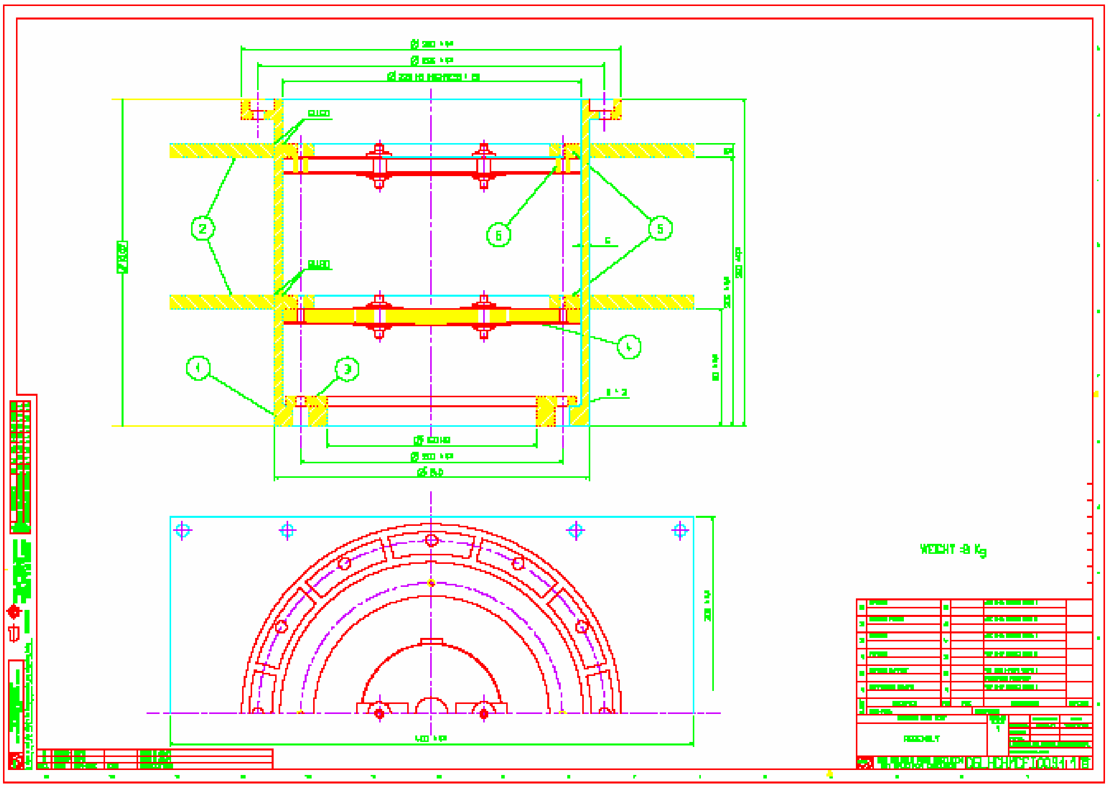

Stresses calculations
4 different types of post

Appendix 10

		Fz axial 100 kN Fy lateral 0 kN	**Fz axial 100 kN Fy lateral 50 kN**	**Fz axial 26 kN Fy lateral 0 kN**	**Fz axial 26 kN Fy lateral 50 kN**	**Fz axial 0 kN Fy lateral 50 kN**
Post characteristics		**Max Stresses in MPa**	**Max Stresses in MPa**	**Max Stresses in MPa**	**Max Stresses in MPa**	**Max Stresses in MPa**
H = 250 mm	Von Mises	28.0	49.6	7.3	44.3	40.2
D = 250 mm	Sig z -	-30.8	-71.5	-8.0	-49.3	-41.3
e = 6 mm	Sigz +	3.2	19.1	0.8	33.4	41.3
H = 250 mm	Von Mises	37.7	97.4	10.9	65.0	60.9
D = 250 mm	Sig z -	-47.6	-108.2	-11.9	-72.1	-60.7
e = 4 mm	Sigz +	7.5	31.0	1.9	48.9	60.7
H = 207 mm	Von Mises	58.0	128.5	13.1	86.0	81.9
D = 200 mm	Sig z -	-63.5	-142.3	-16.5	-95.4	-78.5
e = 3.5 mm	Sigz +	11.0	43.2	2.9	62.5	78.5
H = 192 mm	Von Mises	54.1	115.0	14.1	81.3	80.3
D = 200 mm	Sig z -	-59.0	125.0	-15.3	-81.1	-65.6
e = 3.5 mm	Sigz +		13.9		50.4	65.6

VON MISES EQUIVALENT STRESS - 6.0 mm THICKNESS
100 kN COMPRESSION - 50 kN LATERAL FORCE

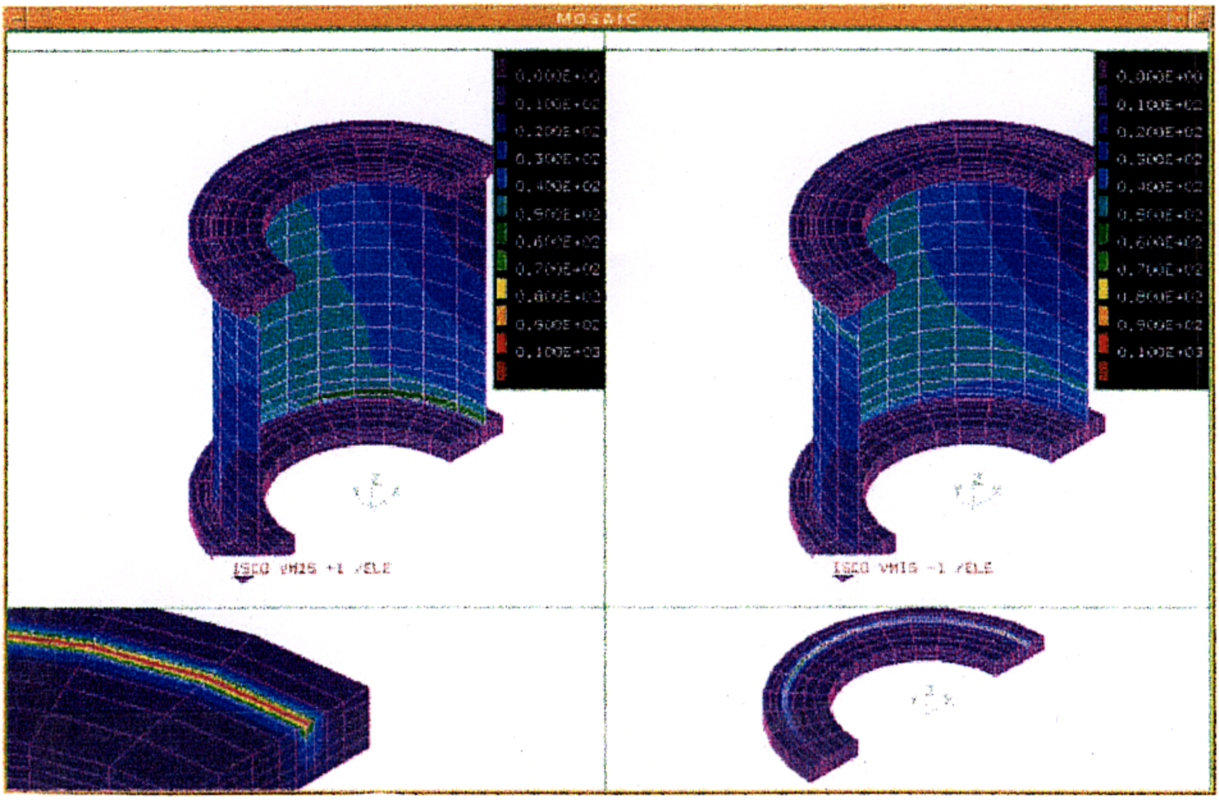

VON MISES EQUIVALENT STRESS - 6.0 mm THICKNESS
26 kN COMPRESSION - 50 kN LATERAL FORCE

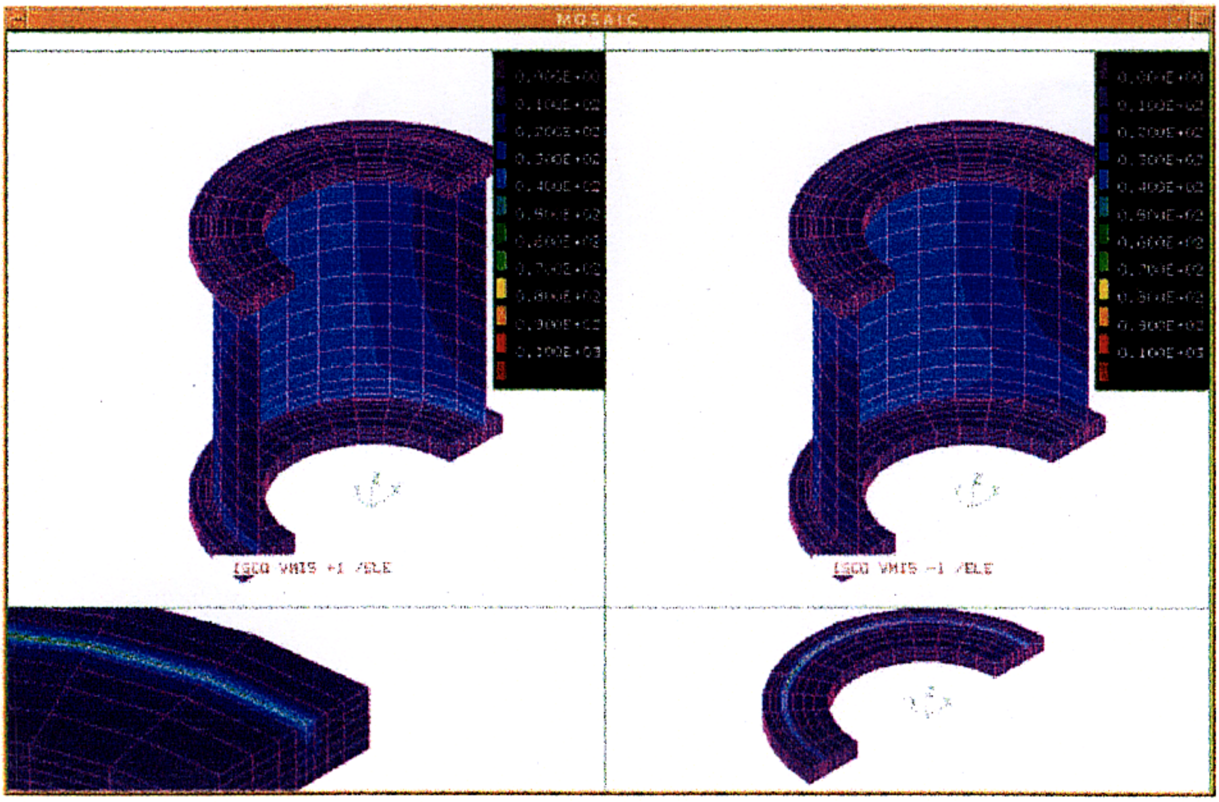

FOOT H=250 mm

VON MISES EQUIVALENT STRESS - 4.0 mm THICKNESS
100 kN COMPRESSION - 50 kN LATERAL FORCE

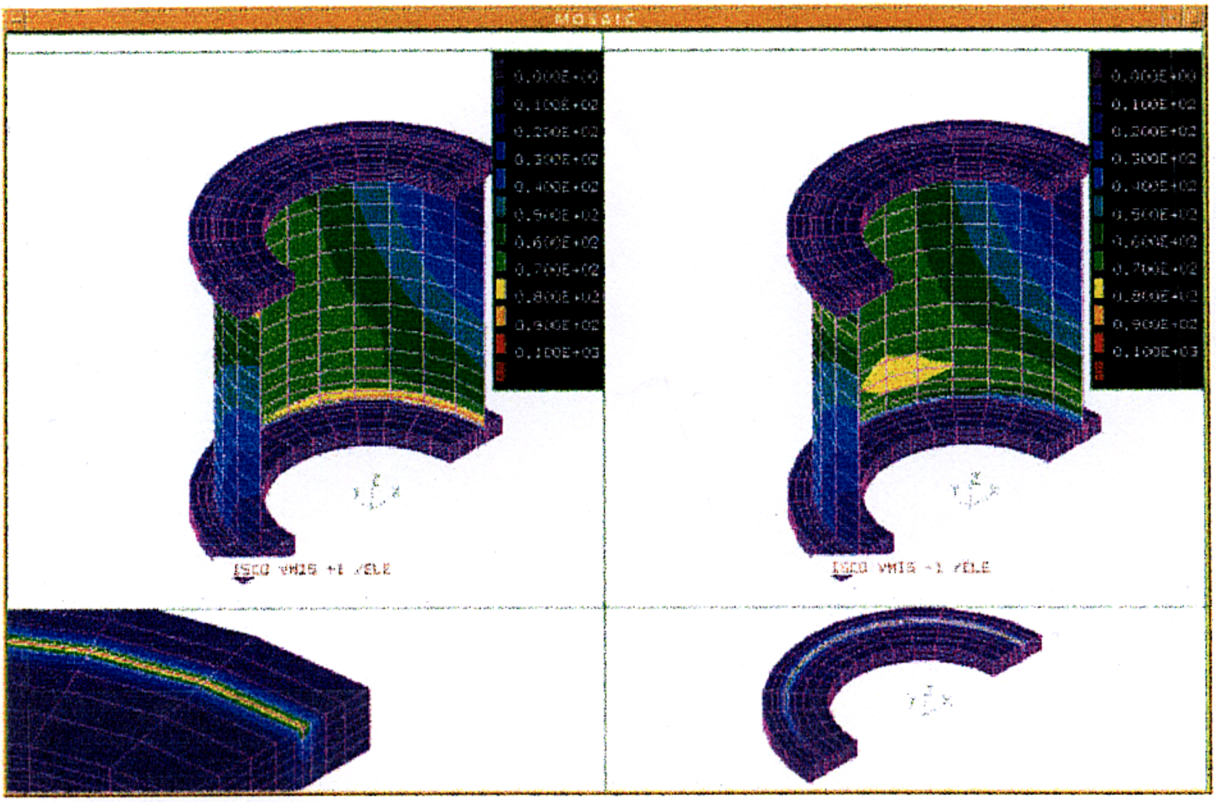

VON MISES EQUIVALENT STRESS - 4.0 mm THICKNESS
26 kN COMPRESSION - 50 kN LATERAL FORCE

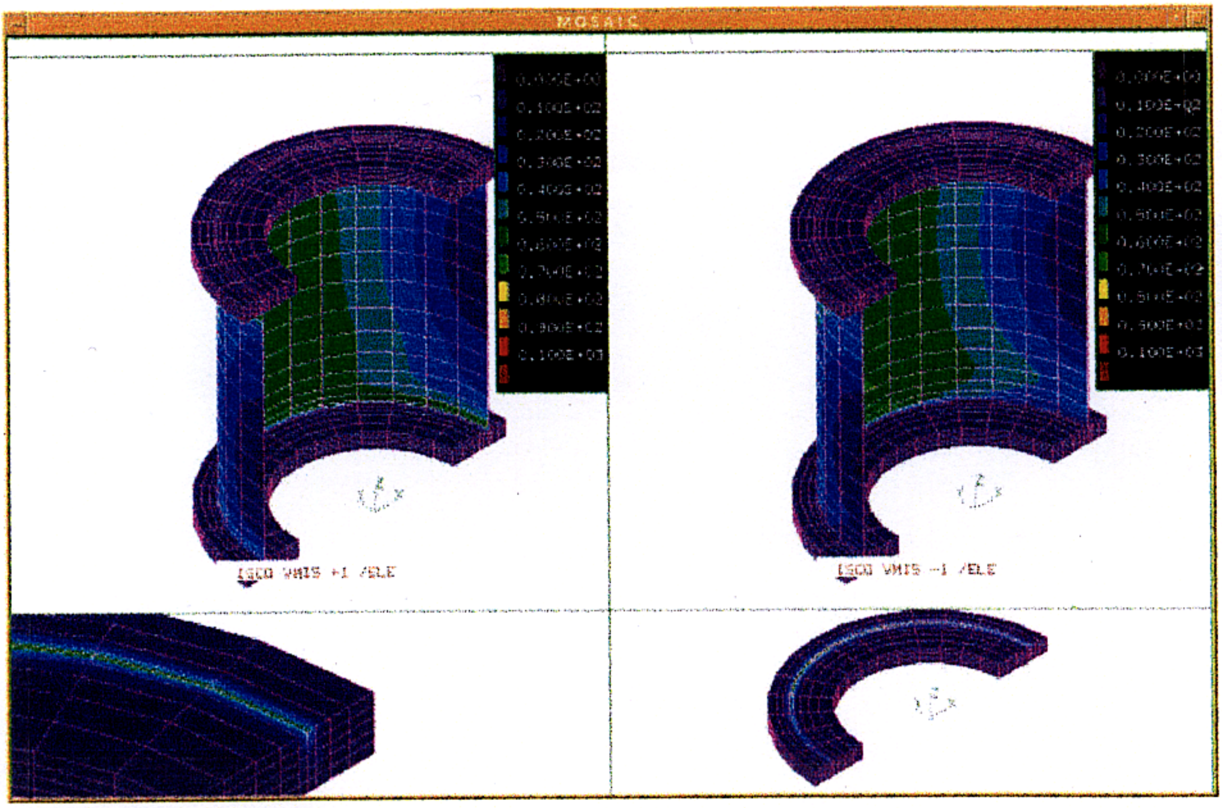

FOOT H=250 mm

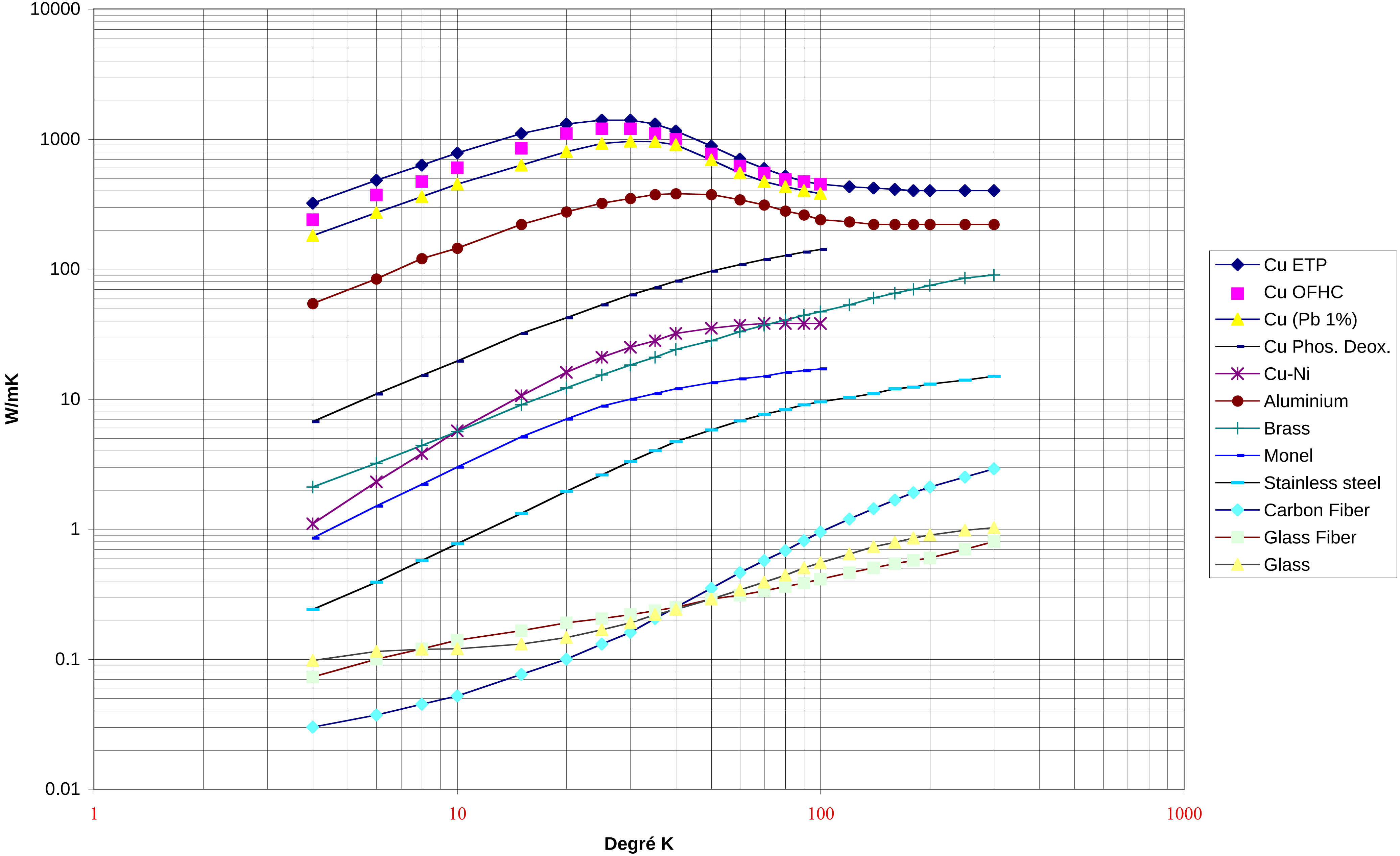
10000
1000
100
10
1
0.1
0.01
W/mK
1
10
100
1000
Degré K
Cu ETP
Cu OFHC
Cu (Pb 1%)
Cu Phos. Deox.
Cu-Ni
Aluminium
Brass
Monel
Stainless steel
Carbon Fiber
Glass Fiber
Glass

Conductive thermal losses in LHC dipole cold foot

Thickness 4 mm **Glassfibre** **Lambda= 0,0691054 + 0,0041207 T - 0,0000059 T^2**

Outer diameter 240 MM **Overall Height 210 MM**

Data	Units	G10 Warp 4 Linear Interpol.	G10 Warp 4 Integration on Lambda
T1	°K	2.0	2.0
T2	°K	6.0	6.0
Lambda(T1)	J/ms°K	0.032	0.077
Lambda(T2)	J/ms°K	0.100	0.094
Lambda moyen	J/ms°K	0.066	
S	M2	0.003	0.003
L1	M	0.015	0.015
Delta T	°K	4.0	4.0
W	Watts	0.052	0.068
Cold foot contribution		2.47%	
Data	Units	G10 Warp 4 Linear Interpol.	G10 Warp 4 Integration on Lambda
T2	°K	6.0	6.0
T3	°K	80.0	80.0
Lambda(T2)	J/ms°K	0.100	0.094
Lambda(T3)	J/ms°K	0.385	0.392
Lambda moyen	J/ms°K	0.243	
S	M2	0.003	0.003
L2	M	0.075	0.075
Delta T	°K	74.0	74.0
W	Watts	0.710	0.681
Cold foot contribution		17.12%	
T3	°K	80.0	80.0
T4	°K	300.0	300.0
Lambda(T3)	J/ms°K	0.385	0.392
Lambda(T4)	J/ms°K	0.800	0.774
Lambda moyen	J/ms°K	0.593	
S	M2	0.003	0.003
L3	M	0.070	0.070
Delta T	°K	220.0	220.0
W	Watts	5.522	5.735
Cold foot contribution		21.03%	
Total loss per foot	Watts	6.28	6.48

Objective/15 M Magnet
Losses in watts

1,8 à 4,2	0.15
4,2 à 77	1.50
77 à 293	15.00

Balance for 11 feet
for one half-cell
0.57 watts
for 1,9 K

Yellow book, feet excluded
for one half-cell
22.70 watts
for 1,9 K

Balance for 11 feet
for one half-cell
7.81 watts
for 4,5-20 K

Yellow book, feet excluded
for one half-cell
37.80 watts
for 4,5-20 K

Balance for 11 feet
Conduct + Radiation(1.5w)
for one half-cell
77.25 watts
for 4,5-20 K

Yellow book, feet excluded
for one half-cell
290.00 watts
for 4,5-20 K

Reminder: for a 10 meter magnet,it was 0,1-1- et 10 watts respectively

Loss=Lambda*Surface*Delta T/Length

Lambda in W/m°K

Composite height 160 mm

1W/m°K=0,86Kcal/mh°C

Foot total height 210 mm,for cryostat 914 mm OD

Conductive thermal losses in LHC 10 m dipole cold foot				**Per foot !!!**	
Thickness 4 mm	**Glass**	**Lambda= 0,0691054 + 0,0041207 T - 0,0000059 T2**			
Thickness 4 mm	**Carbon**	**Lambda=-0,04626026 + 0,00942398 T +0,00000212 T2**			
Data	**Units**	**CARBON 4 Linear Interpol.**	**CARBON 4 Integration on Lambda**	**Objective per foot Losses in Watts**	
T1	**°K**	**2.0**	**2.0**	**1,8 à 4,2**	**0.10**
T2	**°K**	**6.0**	**6.0**	**4,2 à 77**	**1.00**
Lambda(T1)	**J/ms°K**	**0.022**	**-0.027**	**77 à 293**	**10.00**
Lambda(T2)	**J/ms°K**	**0.037**	**0.010**		
Lambda moyen	**J/ms°K**	**0.030**			**As specified**
S	**M2**	**0.003**	**0.003**		**19/1/90**
L1	**M**	**0.020**	**0.020**		
Delta T	**°K**	**4.0**	**4.0**		
W	**Watts**	**0.0172**	**-0.005**		
Foot contribution/ data 1990		**17%**	**-5%**		
Data	**Units**	**CARBON 4 Linear Interpol.**	**CARBON 4 Integration on Lambda**		
T2	**°K**	**6.0**	**6.0**		
T3	**°K**	**80.0**	**80.0**		
Lambda(T2)	**J/ms°K**	**0.100**	**0.094**		
Lambda(T3)	**J/ms°K**	**0.360**	**0.361**		
Lambda moyen	**J/ms°K**	**0.230**			
S	**M2**	**0.003**	**0.003**		
L2	**M**	**0.076**	**0.076**	**Objective per foot**	
Delta T	**°K**	**74.0**	**74.0**	**Losses in Watts**	
W	**Watts**	**0.653**	**0.661**	**1,8 à 4,2**	**0.05**
Foot contribution/ data 1990		**65%**	**66%**	**4,2 à 77**	**0.50**
T3	**°K**	**80.0**	**80.0**	**77 à 293**	**5.00**
T4	**°K**	**300.0**	**300.0**		
Lambda(T3)	**J/ms°K**	**0.360**	**0.361**		**As specified**
Lambda(T4)	**J/ms°K**	**0.800**	**0.774**		**14/1/92**
Lambda moyen	**J/ms°K**	**0.580**			
S	**M2**	**0.003**	**0.003**		
L3	**M**	**0.080**	**0.080**		
Delta T	**°K**	**220.0**	**220.0**		
W	**Watts**	**4.650**	**4.933**		
Foot contribution/ data 1990		**47%**	**49%**		
Total loss/foot	**Watts**	**5.32**	**5.59**		

Loss=Lambda*Surface*Delta T/Length		**Lambda en W/m°K**
Composite height	**0.176**	**1W/m°K=0,86Kcal/mh°C**

In 1992,the thermal budget on feet is 0,1 watt , 1 watt , 10 watts max per magnet

Appendix 16

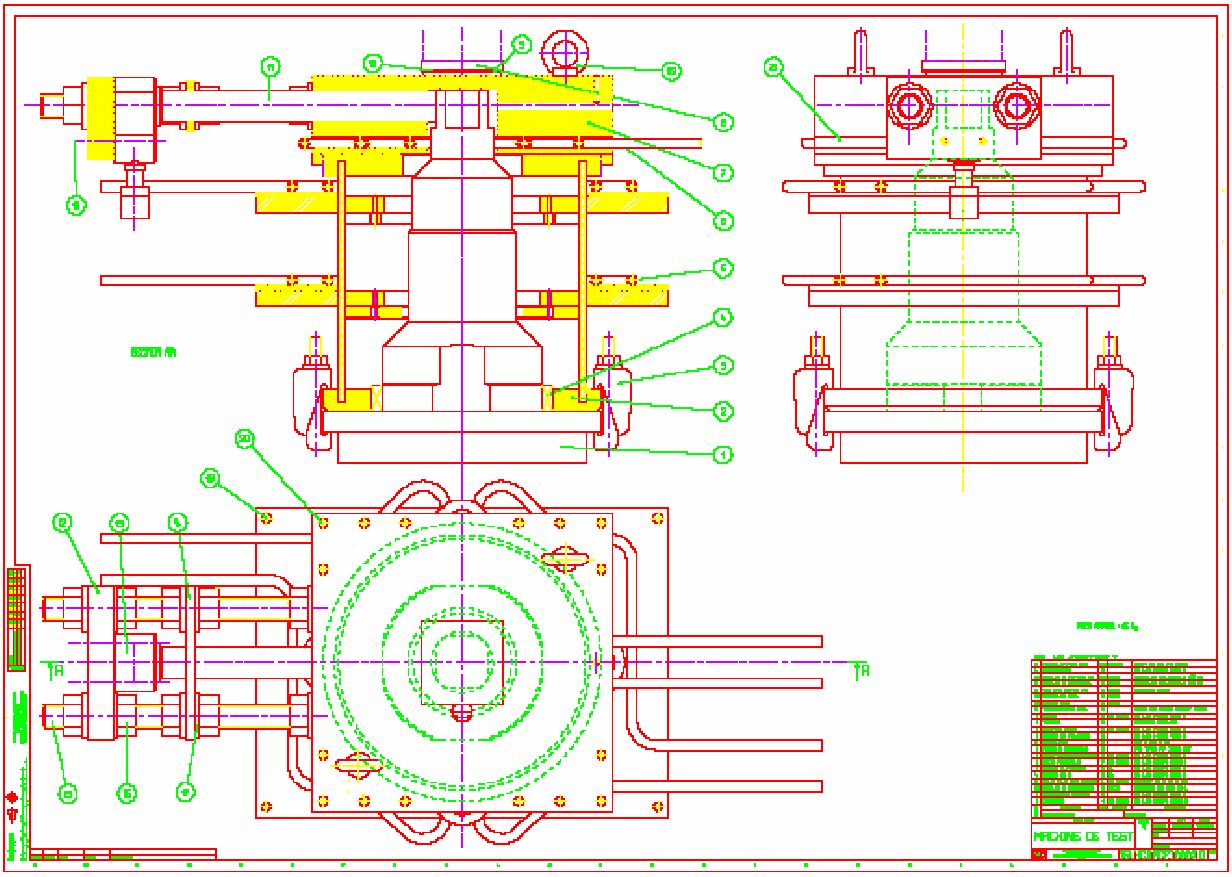

DEFORMATIONS	***Fz = 100 kN***	***Fz = 100 kN***	***Fz = 26 kN***
		Fy = 50 kN	***Fy = 50 kN***
	Compression	**Compression/Flexion**	**Compression/Flexion**
Foot type	**Deflection z direction mm**	**Deflection y direction mm**	**Deflection y direction mm**
Filament winding 6 mm	0,22	0,90	1,00
Filament winding 4 mm	0,23	1,56	1,77
Glass sheet moulded 4 mm	0,62	1,87	2,75
Carbon/glass sheet moulded 4 mm	0,54	1,95	2,53
Resin Transfer M 4 mm	0,57	1,63	1,85
Ultem 6 mm	0,63	3,00	3,72
Isaryl 6 mm	0,96	Rupture /	/
Peek 6 mm			/ Rupture

STRESSES	***Fz = 100 kN***	***Fz = 100 kN***	***Fz = 26 kN***
		Fy = 50 kN	***Fy = 50 kN***
	Compression	**Compression/Flexion**	**Compression/Flexion**
Foot type	**Max Stress (MPa)**	**Max Stress (MPa)**	**Max Stress (MPa)**
Filament winding 6 mm	22.70	62.10	47.80
Filament winding 4 mm	34.30	96.10	73.90
Glass sheet moulded 4 mm	33.70	92.00	78.80
Carbon/glass sheet moulded 4 mm	33.70	93.20	72.80
Resin Transfer M 4 mm	33.70	93.40	77.60
Ultem 6 mm	22.70	67.20	50.30
Isaryl 6 mm	22.70	Rupture	/
Peek 6 mm	22.70		

Appendix 18

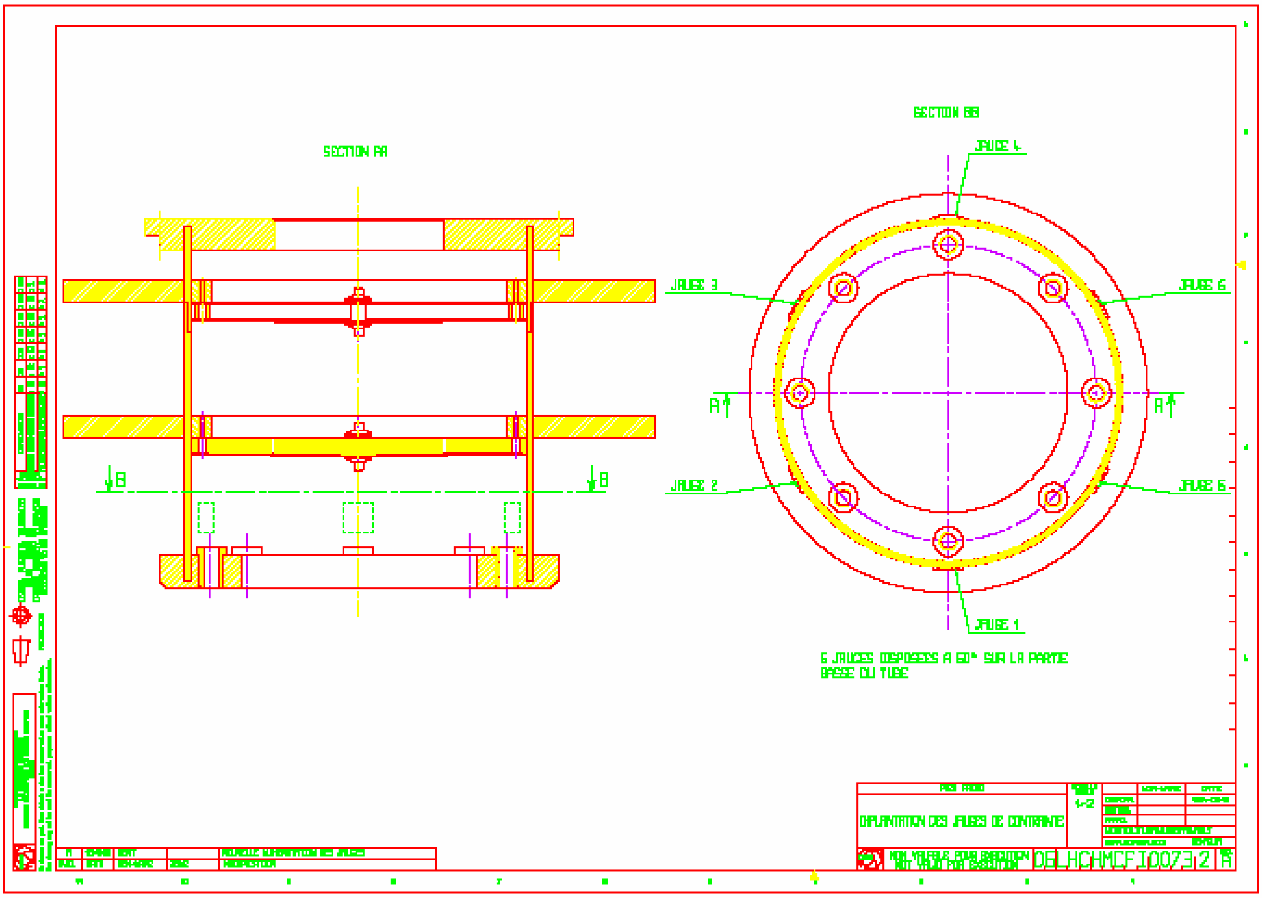
SECTION AA
SECTION BB
JAUGE 4
JAUGE 3
JAUGE 5
JAUGE 2
JAUGE 6
JAUGE 1
A
A
B
B
6 JAUGES DISPOSEES A 60° SUR LA PARTIE BASSE DU TUBE
PAS FROID
IMPLANTATION DES JAUGES DE CONTRAINTE
1-2
NON VALABLE POUR EXECUTION
NOT VALID FOR EXECUTION
06LHCHMCFI0073 2
A
NOUVELLE NUMEROTATION DES JAUGES

Appendix 19

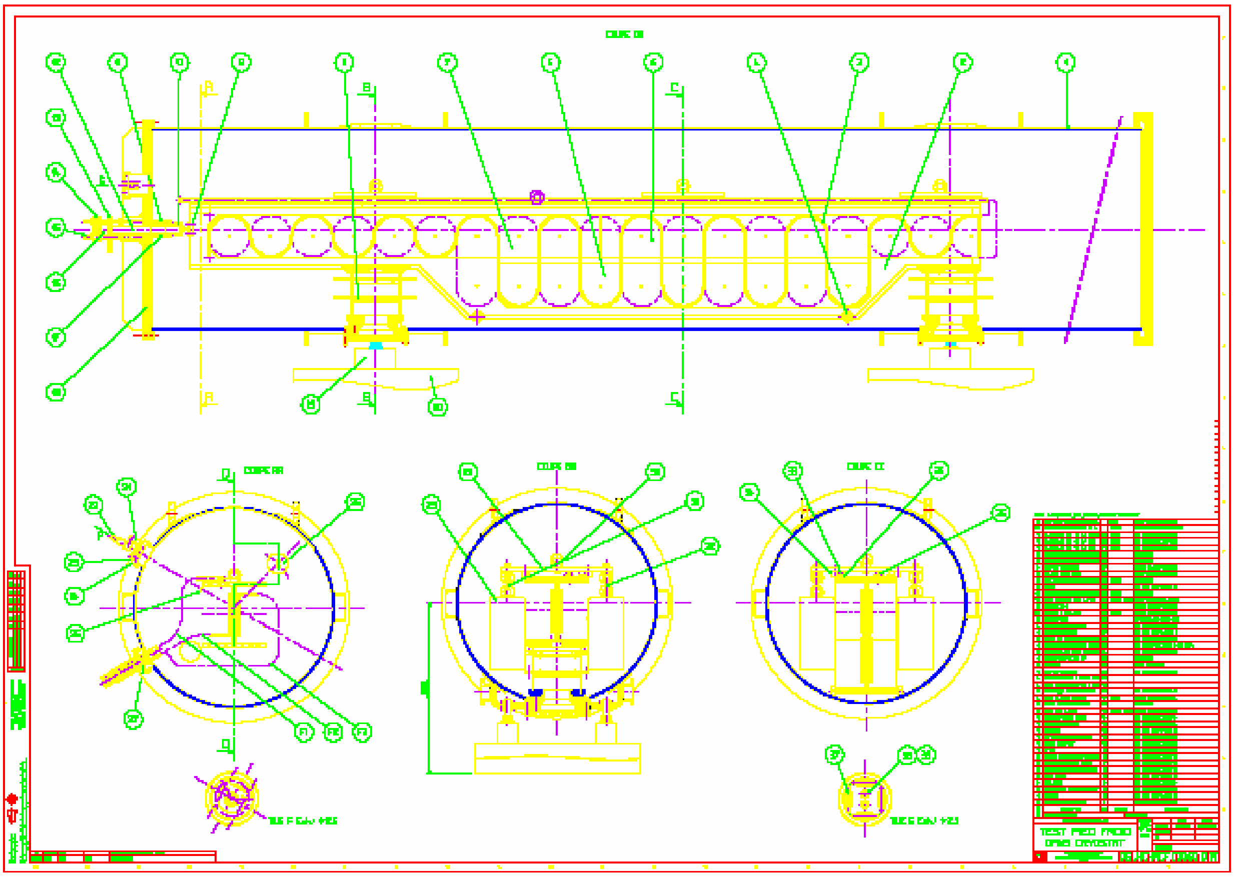
COUPE DD
COUPE AA
COUPE BB
COUPE CC
TEST FEED FROM
DFBA CRYOSTAT

Thermal contraction integer for various materials

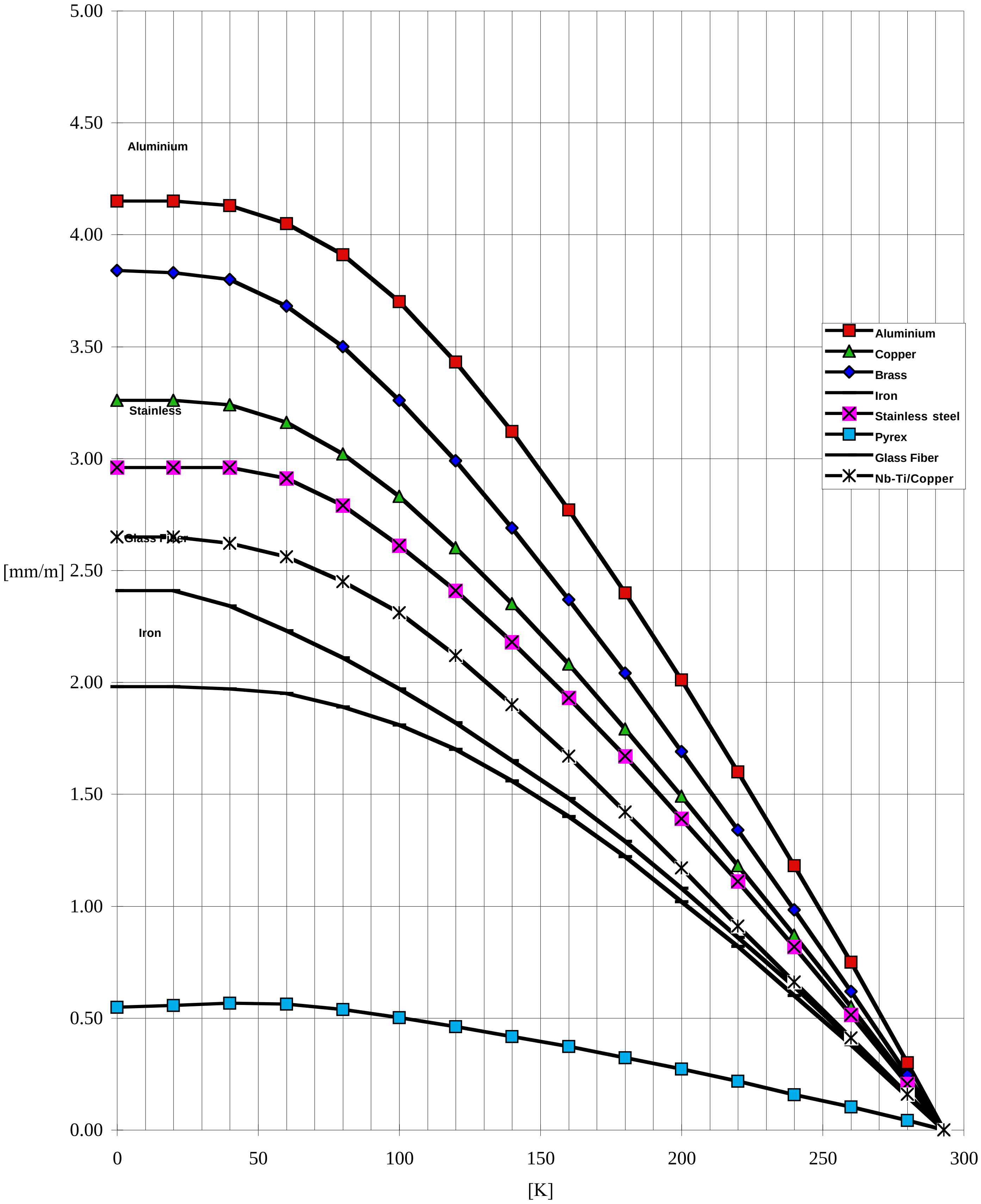

Appendix 21

Compression 24 kN Flexion 50 kN

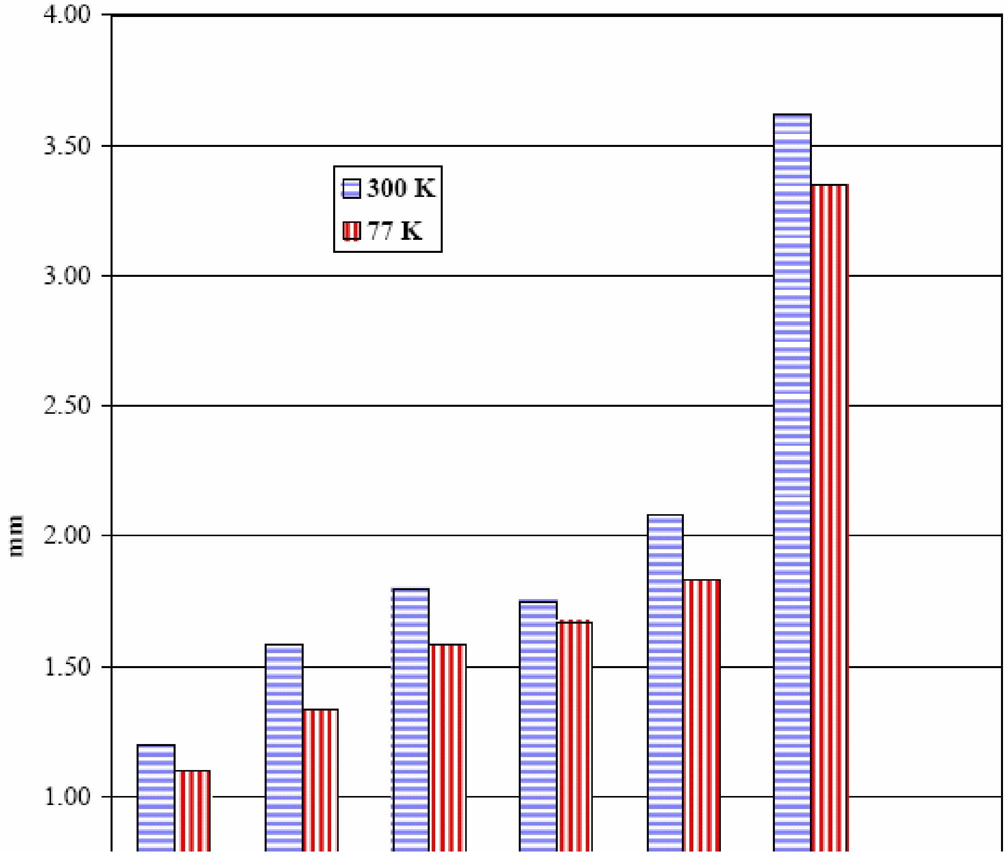

Appendix 22

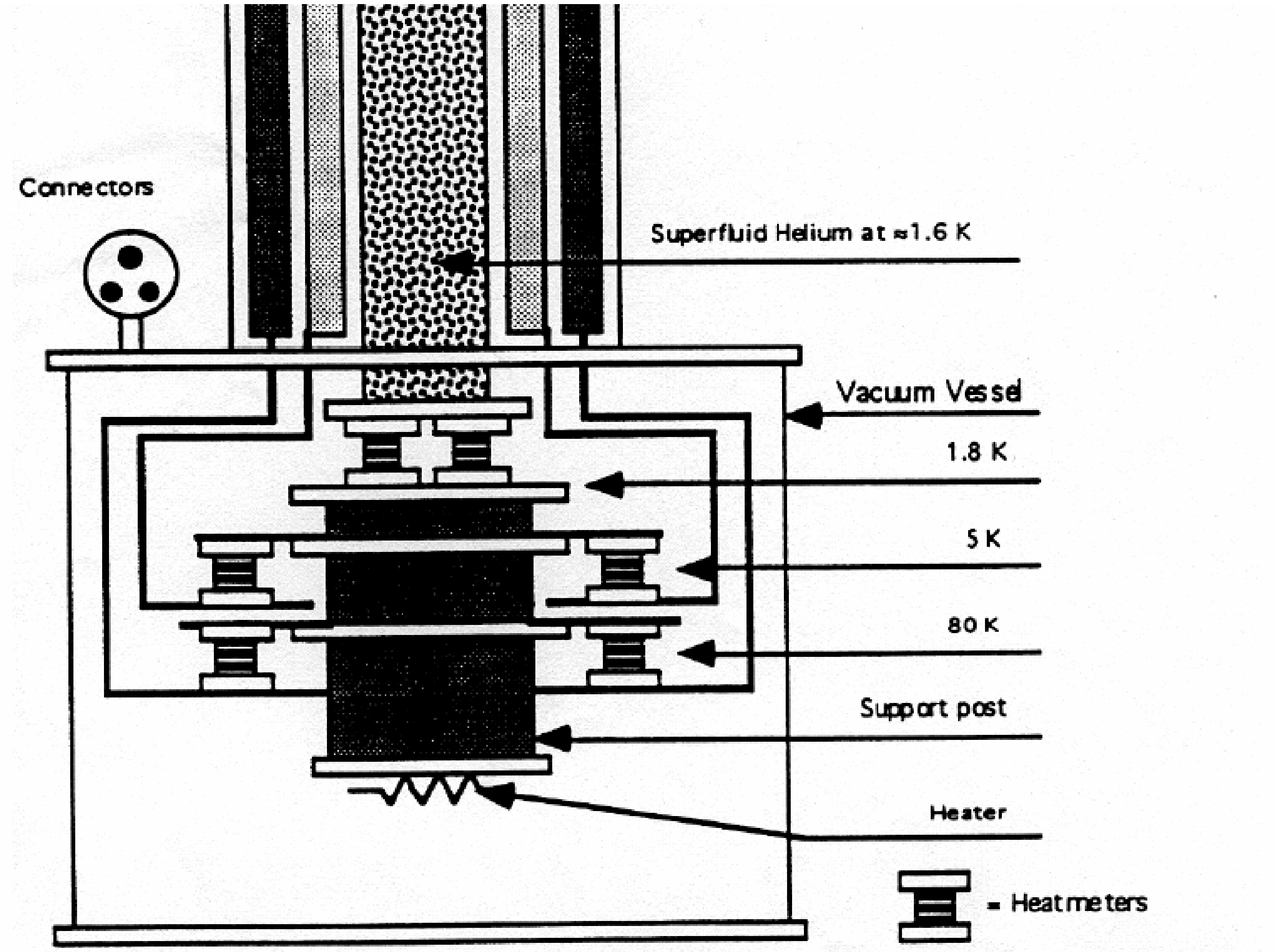
Connectors
Superfluid Helium at ≈1.6 K
Vacuum Vessel
1.8 K
5 K
80 K
Support post
Heater
= Heatmeters

Appendix 23

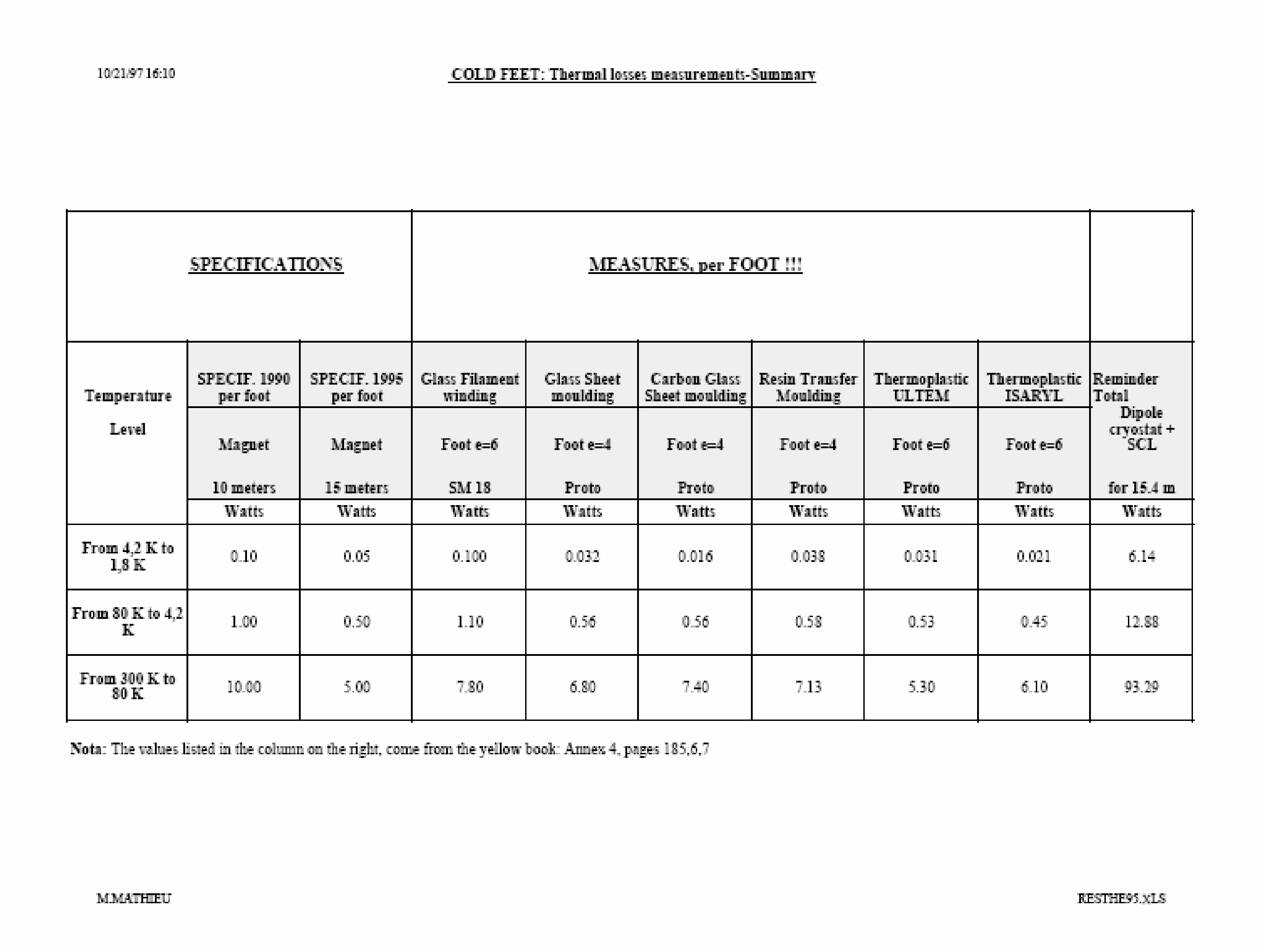

10/21/97 16:10

COLD FEET: Thermal losses measurements-Summary

SPECIFICATIONS			**MEASURES, per FOOT !!!**						
Temperature Level	**SPECIF. 1990 per foot**	**SPECIF. 1995 per foot**	**Glass Filament winding**	**Glass Sheet moulding**	**Carbon Glass Sheet moulding**	**Resin Transfer Moulding**	**Thermoplastic ULTEM**	**Thermoplastic ISARYL**	**Reminder Total Dipole cryostat + SCL**
	Magnet **10 meters**	**Magnet** **15 meters**	**Foot e=6** **SM 18**	**Foot e=4** **Proto**	**Foot e=4** **Proto**	**Foot e=4** **Proto**	**Foot e=6** **Proto**	**Foot e=6** **Proto**	**for 15.4 m**
	Watts	Watts	Watts	Watts	Watts	Watts	Watts	Watts	Watts
From 4,2 K to 1,8 K	0.10	0.05	0.100	0.032	0.016	0.038	0.031	0.021	6.14
From 80 K to 4,2 K	1.00	0.50	1.10	0.56	0.56	0.58	0.53	0.45	12.88
From 300 K to 80 K	10.00	5.00	7.80	6.80	7.40	7.13	5.30	6.10	93.29

Nota: The values listed in the column on the right, come from the yellow book: Annex 4, pages 185,6,7

M.MATHIEU

RESTHE95.XLS

Appendix 24

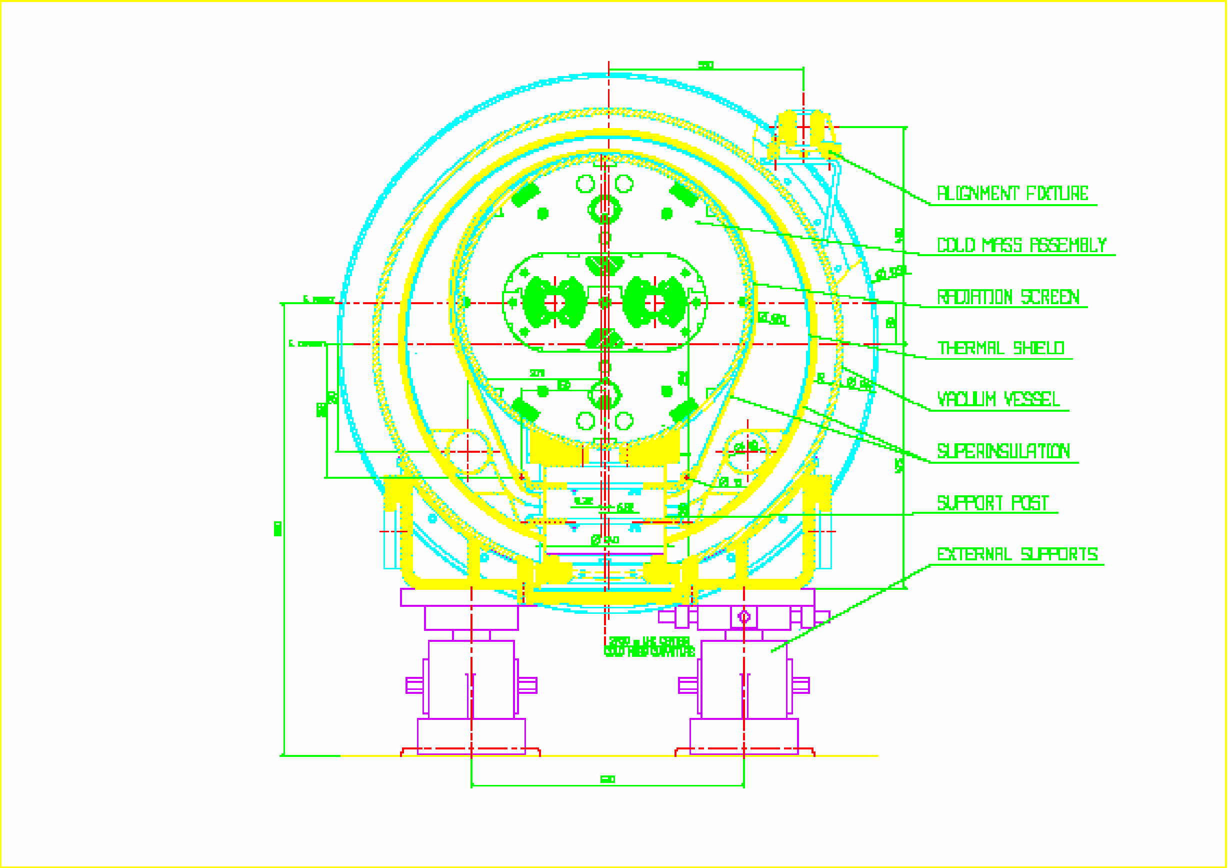
ALIGNMENT FIXTURE
COLD MASS ASSEMBLY
RADIATION SCREEN
THERMAL SHIELD
VACUUM VESSEL
SUPERINSULATION
SUPPORT POST
EXTERNAL SUPPORTS